

## Yaw Angle Effect on the Aerodynamic Performance of Hatchback Vehicle Fitted with Combo-Type Spoiler

Open  
Access

Kwang-Yhee Chin<sup>2</sup>, See-Yuan Cheng<sup>1,2,\*</sup>, Shuhaimi Mansor<sup>3</sup>

<sup>1</sup> Centre for Advanced Research on Energy, Universiti Teknikal Malaysia Melaka, Hang Tuah Jaya, 76100 Durian Tunggal, Melaka, Malaysia

<sup>2</sup> Faculty of Mechanical Engineering, Universiti Teknikal Malaysia Melaka, Hang Tuah Jaya, 76100 Durian Tunggal, Melaka, Malaysia

<sup>3</sup> Faculty of Mechanical Engineering, Universiti Teknologi Malaysia, 81310 UTM Skudai, Johor, Malaysia

### ARTICLE INFO

### ABSTRACT

#### Article history:

Received 5 February 2018

Received in revised form 12 March 2018

Accepted 20 March 2018

Available online 15 April 2018

This study investigated the effect of yaw angle on the aerodynamic performance of hatchback vehicle model fitted with a spoiler featuring a configuration combining the wing and strip spoiler designs. To date, majority of the tests performed on spoilers were done in a straight-ahead driving condition. However, the effect of spoiler is most demanded during cornering for stability reason. A RANS-based Computational Fluid Dynamics (CFD) method was used to simulate the flow. Validation of the method was carried out by comparing the numerically obtained results with the experimental data. The findings show that both the drag coefficient,  $C_d$ , and lift coefficient,  $C_l$  had increased when the vehicle was subjected to higher yaw angle. The wing part of the spoiler did performed in favour of reducing the  $C_l$ , but its contribution to the overall  $C_l$  was only about 4.28%. The main body parts contributed to the decrease in  $C_d$  and  $C_l$  are the front and underbody, respectively.

#### Keywords:

Spoiler, hatchback, yaw angle, aerodynamics, CFD

Copyright © 2018 PENERBIT AKADEMIABARU - All rights reserved

## 1. Introduction

Basically, rear spoiler is an aerodynamic device added externally to the trailing edge of the roof or trunk of a vehicle to alter the air movement around the vehicle. Ever since its practicability on racing car has been proven, a variety of spoiler types has been investigated extensively in previous studies [1-10]. Generally, there are two types of rear spoilers, namely strip-type and wing-type spoilers. Besides, there are spoilers in the market nowadays featuring the combination of the two configurations. This type of spoiler will be designated as combo-type spoiler (or combo spoiler) for convenient in the discussions in this study.

The effectiveness of spoilers has been the interest in various studies due to fuel and energy consumption, vehicle stability, and racing speed concerns. Besides, every measure should be taken to minimize the danger posed by vehicles [11]. However, publication on the effectiveness of combo-type spoiler made available to the public was scarce. Despite the scarcity, there was a study

\* Corresponding author.

E-mail address: [cheng@utem.edu.my](mailto:cheng@utem.edu.my) (See-Yuan Cheng)

on this type of spoiler reported by Gerhardt and Kramer [12] on the aerodynamic optimization of a Group-5 racing car. The result published shows a 30s reduction of lap time on Nürburgring racing track. In this study, the results reported are produced using wind tunnel experimentation and practical experience. Hence there was no specific data recorded on how the spoiler contributed to the reduced lap time.

Moreover, although yaw angle influences the aerodynamic performance of vehicles, as shown in previous studies [13-14], majority of the studies on rear spoilers did not reported on this influences. To fill in the gap, the present study investigated the aerodynamic performance of the combo-type spoiler in yawing conditions.

## 2. Methodology

### 2.1 Hatchback Model and Spoiler Configuration

In the present study, the wing spoiler utilizes the NACA 0018 profile combine with a strip spoiler using two endplates. The angle of attack of both spoilers is  $5^\circ$ . This spoiler is mounted on a simplified road vehicle geometry, namely Ahmed model. The reason for using a simplified model instead of real vehicle body is to eliminate the interference effect among the body parts which would otherwise found on the real vehicles. This approach has been implemented successfully in many studies concerning automotive aerodynamics (e.g. [15-19]). The details of the dimensions of Ahmed model were based on Ahmed et. al. [16]. The slant angle for this model is  $35^\circ$ , which is a typical angle for most hatchback vehicle. Meanwhile the details of the spoiler were shown in Figure 1. The wing spoiler has a chord length of 69 mm, which is the result of the scale ratio of 6.61% of the length of Ahmed model, resembling the length of wing spoiler in reality. Besides, the sharp end of the wing had been filleted (2 mm radius) to avoid highly skewed cells during meshing. For the same reason, all the sharp edges of the two endplates supporting the wing spoiler were filleted (2 mm radius). The thickness of a single endplate was 5mm.

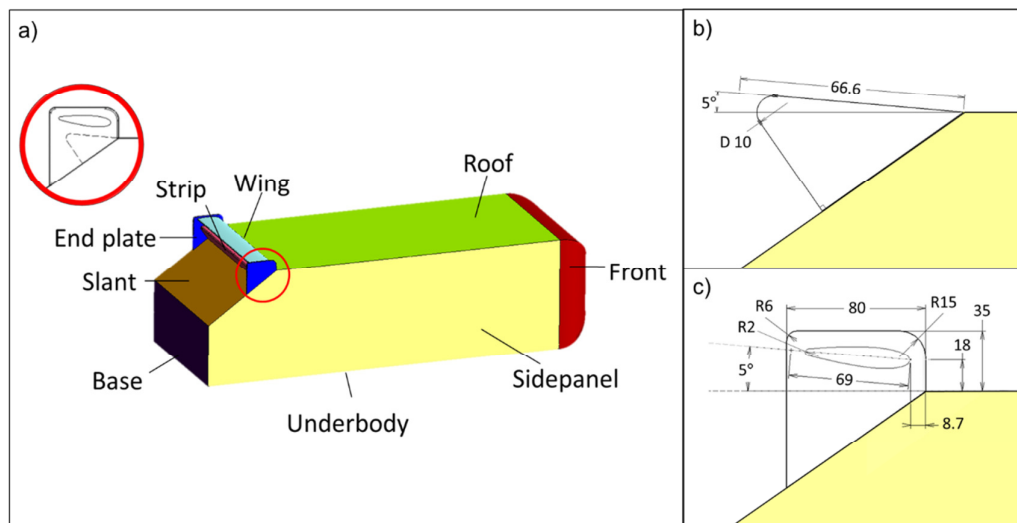


**Fig. 1.** Combo-type spoiler mounted on Ahmed model (a); detailed dimensioning of strip part (b), wing part and endplate (c)

Figure 2 shows the definition of yaw angle applied in this study. The yaw angles investigated are from  $0^\circ$  to  $12^\circ$ , at  $4^\circ$  increments. The maximum yaw angle was fixed at  $12^\circ$  due to the fact that,

according to Cooper [17], vehicle travelling at high speed normally would not experience yaw angle greater than this value.

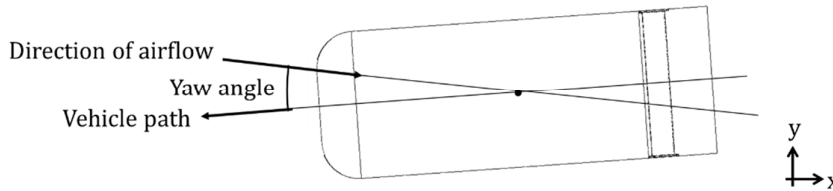


**Fig. 2.** Convention of yaw angle

## 2.2 Computational Method

A numerical simulation method was adopted in this study to inspect the yaw angle effect on the aerodynamic forces of a simplified hatchback vehicle model mounted with a combo spoiler. The commercial finite-volume solver ANSYS Fluent was utilized to obtain all the results in this study. Moreover, Reynolds-averaged Navier-Stokes (RANS) approach was used. Equations 1 and 2 are the governing equations, which are the time-averaged continuity and momentum equations for incompressible Newtonian fluid:

$$\frac{\partial u_i}{\partial x_i} = 0 \quad (1)$$

$$\rho u_j \frac{\partial u_i}{\partial x_j} = \frac{\partial}{\partial x_i} [-p\delta_{ij} + 2\mu S_{ij} - \rho u'_i u'_j] \quad (2)$$

where,

$\rho$	= density of fluid
$u$	= time-averaged velocity
$p$	= time-averaged static pressure
$\mu$	= viscosity of fluid
$S_{ij}$	= mean rate of strain tensor
$\rho u'_i u'_j$	= Reynolds stresses representing the effects of turbulence

The Reynolds stresses term was then modelled using the two-equation turbulence model, namely k-epsilon realizable model. The enhanced wall treatment (EWT) option in the simulation package was used. By using this function, the wall function will be automatically imposed to model the boundary layer profile for estimating the surface friction on the wall surfaces as the first grid point is in the log-layer range. Steady-state simulation was achieved by utilizing steady, pressure-based solver. All the results recorded in the present study were produced using a second-order node-based upwind discretization scheme.

The boundary condition for inlet was set as uniform flow, where the inlet velocity  $U = 40\text{m/s}$  and turbulence intensity of 0.2%. The corresponding Reynolds number (Re) was  $2.7 \times 10^6$  (based on to the model's length).

The computational domain resembling a rectangular box with the two ends set as inlet and outlet. The domain has a cross sectional area of 1450 mm x 3890 mm (height x width). Hence, the blockage ratio obtained was below 2%, which is far lower compared to the typical accepted 5% blockage ratio in automotive aerodynamic testing (Hucho and Sovran [20]). The upstream and downstream of the domain extends for 1.4*l* and 11.5*l* respectively, where *l* is the length of the model. As for the outlet, the pressure outlet boundary condition was used, with the pressure value

set as zero gauge pressure. The remaining walls of the domain were then set as symmetry boundary condition. Meanwhile, the ground and model surfaces were set as no-slip wall.

### 2.2.1 Meshing

The model was meshed with the computational domain being discretized into unstructured and prismatic cells. The result of grid convergence study indicates that the mesh is sufficiently refined at around 2337141 cells. The first prismatic cell layer thickness around the model surface was 0.5 mm. The corresponding  $y^+$  ranges from around 1.2 to 80.

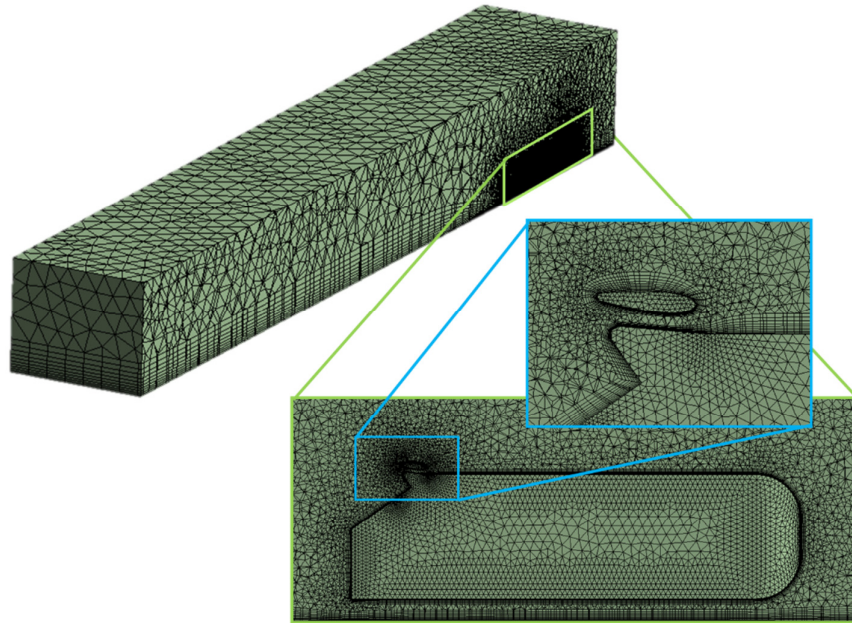


**Fig. 3.** Distribution of mesh density around the model with a close-up of prismatic cells surrounding the spoilers

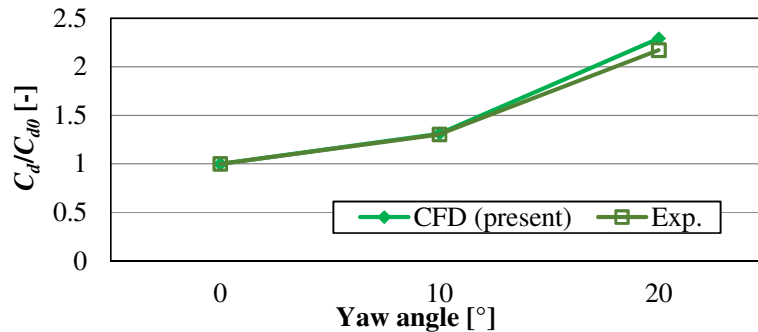
### 2.2.2 Validation

Validation of the numerical method used was done through the effort of reproducing the experimental results published by Bello-Millán *et al.*, [13]. The comparison of the drag coefficient,  $C_d$  of the Ahmed model (with slant angle of  $25^\circ$ ) at increasing yaw angle obtained by the present CFD method and the experimental result by Bello-Millán *et al.*, [13] was shown in Figure 4. As may be seen, the two curves are in very good agreement (with the maximum difference of 5.2% at  $20^\circ$  yaw angle). As mentioned earlier, the present study only covered the yaw angle range up to  $12^\circ$ . Thus, by interpolation, the corresponding percentage difference between the CFD and experimental results at  $12^\circ$  yaw angle is only 0.6%. Therefore, we can conclude that the present CFD method is suitable for the investigation.

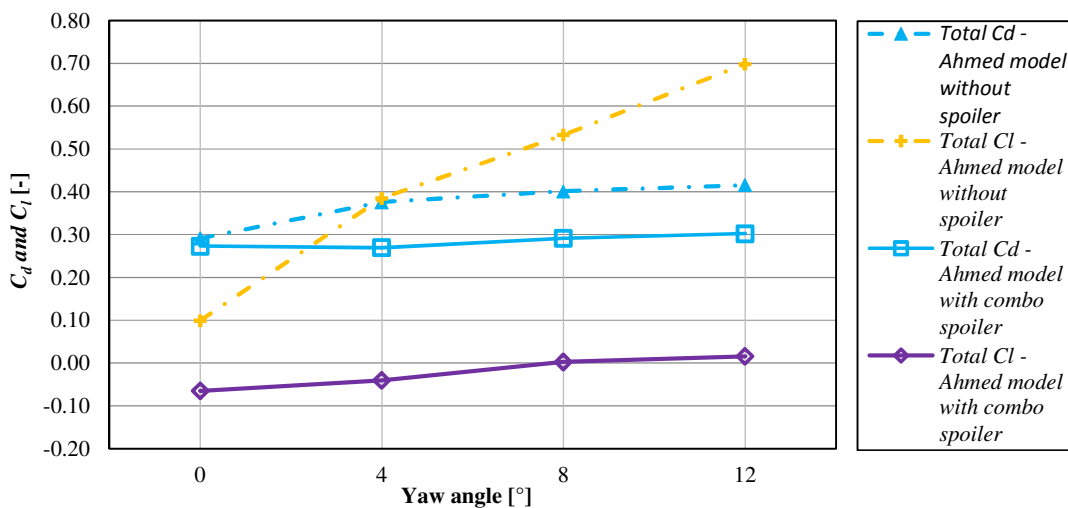
## 3. Results and Discussion

Figure 5 compares the total  $C_d$  and  $C_l$  of the model with and without combo spoiler against yaw angle. As may be seen, all the aerodynamic force coefficients increased with increasing yaw angle. Note that in this study, the  $C_d$  is defined as the component parallel to the longitudinal axis of the

model. The trend of the results suggests the vehicle's overall aerodynamic performance would deteriorate when it is not travelling in a straight path. Moreover, both the  $C_d$  and  $C_l$  of Ahmed model mounted with combo spoiler were lower than that of the  $C_d$  and  $C_l$  recorded for Ahmed model without the spoiler. The reduction of  $C_d$  and  $C_l$  after the addition of combo spoiler reached up to 27.32% and 97.72% respectively. In addition, the increase in both the aerodynamic force coefficients was also lowered at increasing yaw angle. Such phenomenon was remarkably showed in the increase of  $C_l$ . In particular, the  $C_l$  has increased by about 604% in the case without the spoiler when the yaw angle increased from  $0^\circ$  to  $12^\circ$  yaw. However, the  $C_l$  increment in the with-sp spoiler case was only 124.49%.



**Fig. 4.** Effect of yaw angle on the  $C_d$  of Ahmed model obtained by the present CFD and the experimental work of Bello-Millán *et al.* [13]; The  $C_d$  values by each method are normalized by their respective  $C_d$  values at  $0^\circ$  yaw



**Fig. 5.** Yaw angle effect on the  $C_d$  and  $C_l$  of Ahmed model with and without the combo spoiler

In Figure 6, we examine the effect of yaw angle on the  $C_d$  and  $C_l$  of each component (i.e. the wing and strip parts) of the combo spoiler separately. The  $C_d$  for both the wing and strip parts has an increasing trend. In particular, the increase is about 2.29% and 32.86% at  $12^\circ$  yaw for the wing and strip parts, respectively. As for the  $C_l$ , the strip part has shown an increasing tendency whereas the wing part has shown an opposite tendency. Specifically, when the yaw angle increased to  $12^\circ$ ,  $C_l$

value of the strip part has increased by about 21.62%, whereas the value of the wing part has dropped by about 27.7%. These tendencies indicate that the wing part is an important component in the combo spoiler for controlling the  $C_l$  when the vehicle is travelling in non-zero yaw conditions, despite some drag penalty.

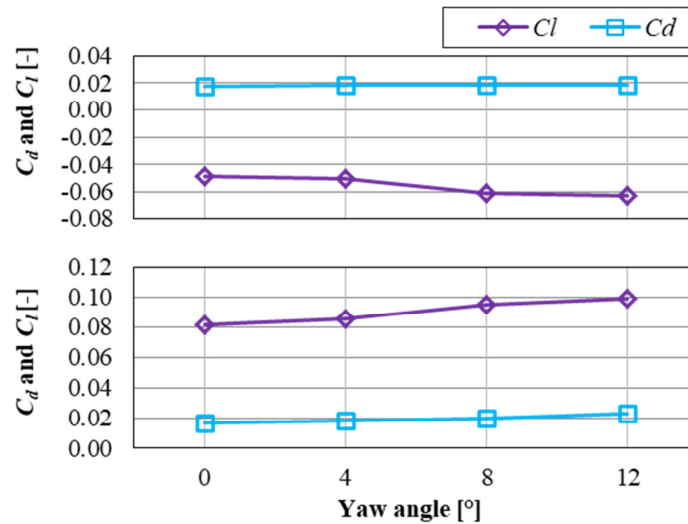


**Fig. 6.** Yaw angle effect on the  $C_d$  and  $C_l$  of the wing and strip parts of the combo spoiler

Figure 7 shows the contribution of each body part to the  $C_d$  and  $C_l$  with increasing yaw angles. At 0° yaw, the  $C_d$  contribution from the wing part is only about 6.53% of the total  $C_d$  of the model. As the yaw angle increases to 12° yaw, the proportion contribution diminishes to 5.87%. On the other hand, the contribution from the strip part was 6.36% at 0° yaw and rose up to 7.47% at 12° yaw.

Meanwhile, in regard to  $C_l$ , only the underbody and wing part of the spoiler had contributed to downforce, whereas the other components had contributed to positive lift. In addition, despite the wing part's positive influence to the overall  $C_l$ , its proportion was only about 4.28% of the overall downforce generated.

### 3.1 Effect of Yaw Angle on Flow Structures

As demonstrated in Figure 8, there were four longitudinal vortices (marked as A, B, C and D) developed from the four front corners of the model when it was subjected to yaw angles. The formation of such vortices is considered reasonable as the front corner edges are of angular shape. Viewing from the back of the model, the vortices A and D are showing a counter-clockwise rotation whereas the vortices B and C are showing a clockwise rotation.

As illustrated, near the windward side, the axes of vortices A and B are located on the top and bottom of the model respectively. Whilst, near the leeward side, the axes of vortices C and D were locating away from the model surfaces. Consequently, when the model was subjected to higher yaw angle, the surface pressure of the model might be influenced by the windward vortices as a result of increasing vortex strength.

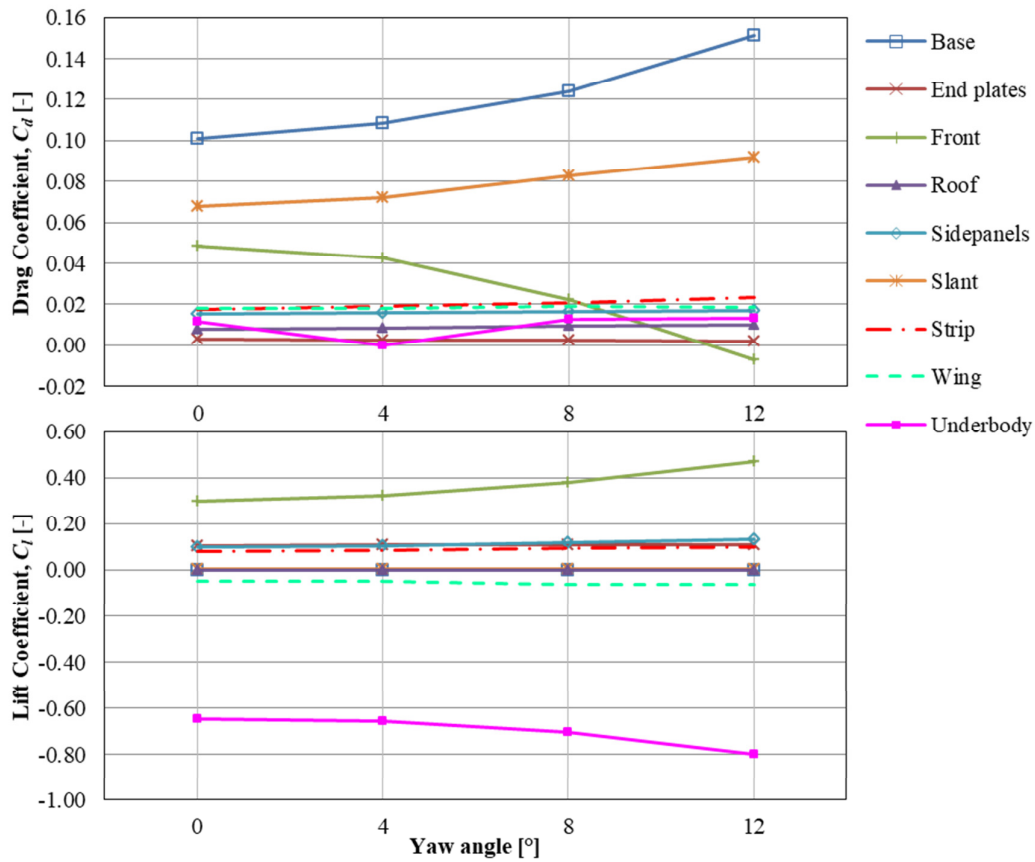


Fig. 7. Contributions of body parts to the  $C_d$  and  $C_l$  with increasing yaw angles

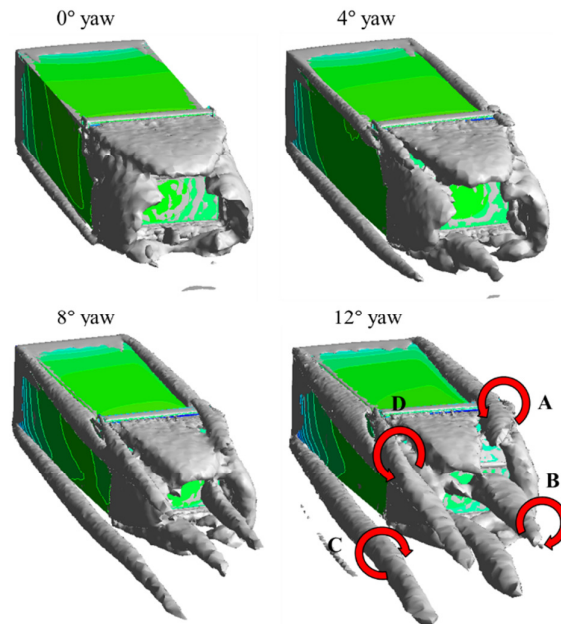
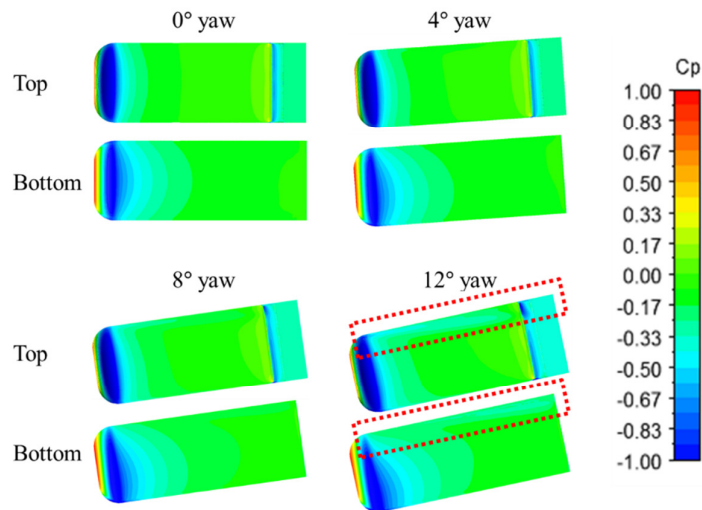


Fig. 8. Vortex structures around the model at different yaw angles; iso-surface of  $Q$  criterion (0°, 4°, 8° and 12°)

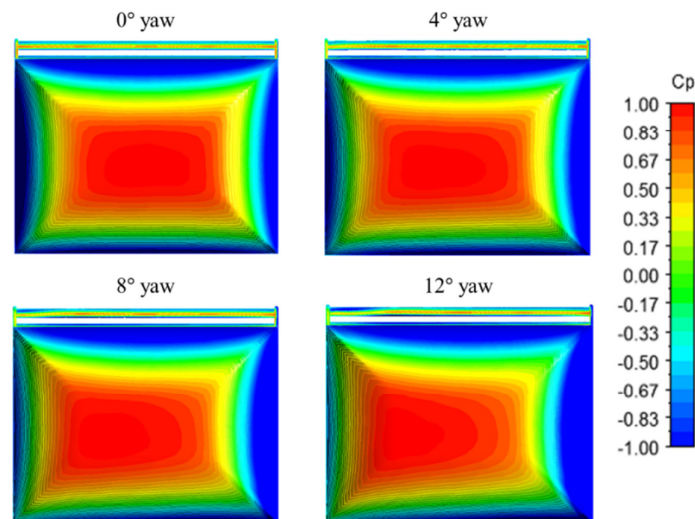
### 3.2 Physical Mechanism

Figure 9 compares the surface pressure distribution on the top and bottom part of the model at different yaw angles. As shown, the top and bottom parts of the model have exhibited the low surface pressure regions (regions in the red boxes) along the windward side due to vortices A and B. On the top part of the model, decreasing in pressure of the roof would cause an increase in the  $C_l$ . Hence, due to such influence, the roof of the model has exhibited an increase in  $C_l$  with increasing yaw angles. In fact, the roof has the highest contribution to the increase in the overall  $C_l$ .

As for the surface pressure at the bottom part of the model, a decrease in the surface pressure would cause a decrease in  $C_l$ . Hence, the underbody has contributed to the decrease in  $C_l$  with increasing yaw angles.



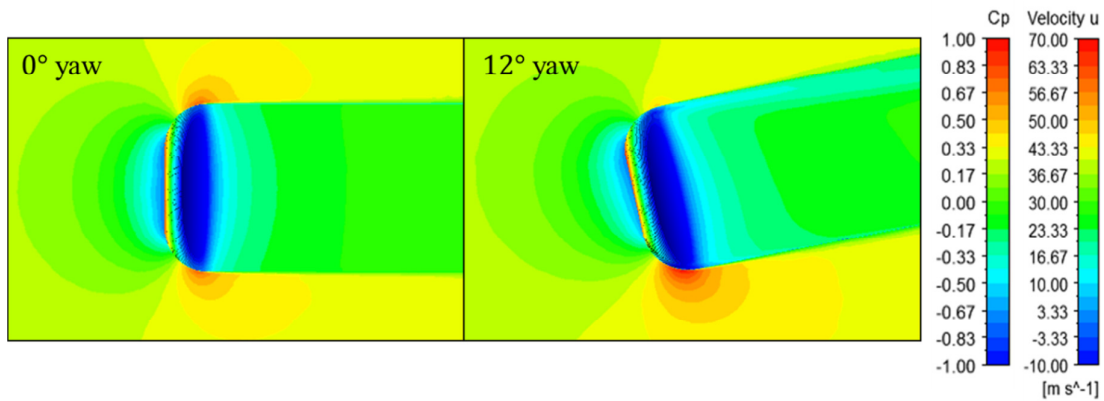
**Fig. 9.** Surface pressure distributions at different yaw angles (top and bottom view)



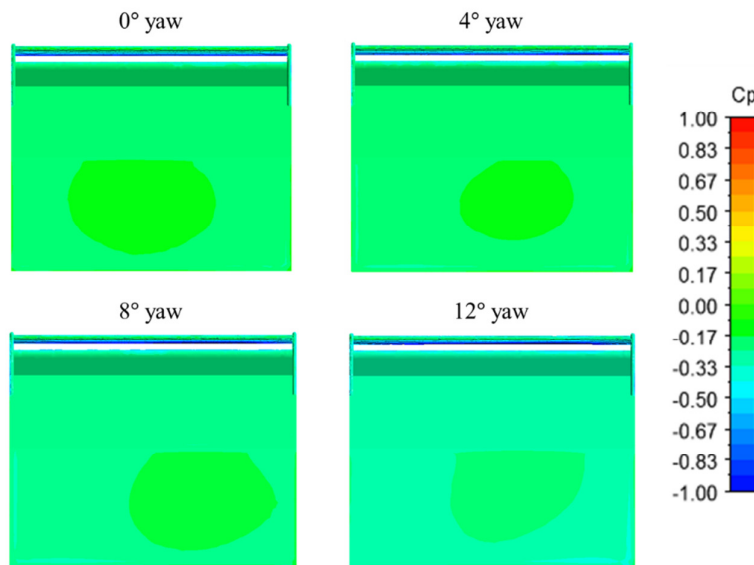
**Fig. 10.** Surface pressure distribution of the front part at different yaw angles (front view)

Figure 10 shows the mechanism of  $C_d$  reduction due to the front part of the model. As may be seen, the low surface pressure region near the leeward side has become wider at higher yaw angle. This phenomenon was caused by the flow acceleration near the leeward side corner at higher yaw angle as shown in Figure 11.

On the other hand, the drop in the surface pressure of the slant and base at higher yaw angles (see Figure 9 and Figure 12) is the reason why the two body parts have contributed to the increase in the model's overall  $C_d$  at higher yaw angles. Their pressure drop is associated to the increase in the size of the separation bubbles at the back of the model at higher yaw angle (see Figure 13).



**Fig. 11.** Yaw angle effect on the velocity distribution near the front part of the model (Top view; visualization plane at the mid height of the model)



**Fig. 12.** Surface pressure distributions at different yaw angles (back view)

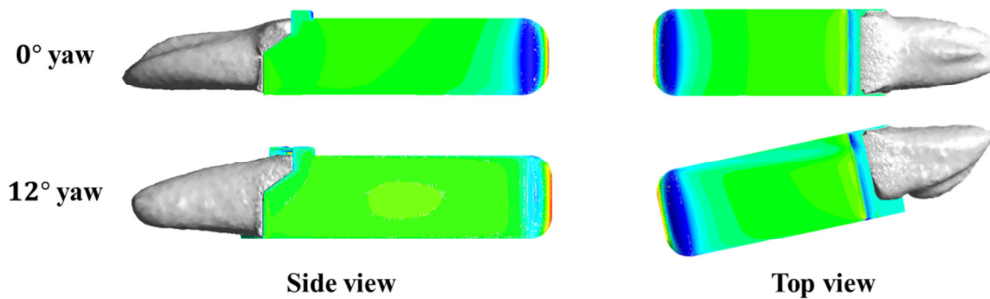


Fig. 13. Separation bubbles formed at different yaw angles; iso-surface of  $u = 0$  m/s

#### 4. Conclusion

The present study investigated the effect of yaw angle on the aerodynamic performance of hatchback vehicle model fitted with a spoiler featuring a configuration combining the wing and strip spoiler designs by a RANS-based CFD method. The results reveal that both the drag and lift coefficients of the simplified vehicle model have increased with increasing yaw angle. In the contexts of fuel economy and drive safety, such tendency is undesirable. However, when compared to the vehicle model without the spoiler, the coefficients have been reduced markedly.

The wing and strip parts of the spoiler have shown different  $C_d$  and  $C_l$  tendencies. In particular, while the  $C_d$  of the two parts increases with yaw angle, only the  $C_l$  of the strip part has shown an increase tendency. The wing part on the other hand has shown an opposite tendency.

The main body parts contributed to the increase in  $C_d$  at higher yaw angles are the base and slant, while the front has contributed to a decrease tendency. Furthermore, the rise in  $C_l$  is caused by the roof while the underbody has imparted an opposite tendency.

#### Acknowledgement

The authors would like to thank Universiti Teknikal Malaysia Melaka (UTeM) and Ministry of Higher Education for supporting this research under FRGS FRGS/1/2015/TK03/FKM/02/F00273.

#### References

- [1] Cheng, S. Y., and S. Mansor. "Rear-roof spoiler effect on the aerodynamic drag performance of a simplified hatchback model." In *Journal of Physics: Conference Series*, vol. 822, no. 1, p. 012008. IOP Publishing, 2017.
- [2] Cheng, See-Yuan, and Shuhaimi Mansor. "Influence of rear-roof spoiler on the aerodynamic performance of hatchback vehicle." In *MATEC Web of Conferences*, vol. 90, p. 01027. EDP Sciences, 2017.
- [3] Daryakenari, Behrang, Shahrir Abdullah, Rozli Zulkifli, E. Sundararajan, and AB Mohd Sood. "Numerical study of flow over ahmed body and a road vehicle and the change in aerodynamic characteristics caused by rear spoiler." *International Journal of Fluid Mechanics Research* 40, no. 4 (2013).
- [4] Kim, Inchul, Hualei Chen, and Roger C. Shulze. *A rear spoiler of a new type that reduces the aerodynamic forces on a mini-van*. No. 2006-01-1631. SAE Technical Paper, 2006.
- [5] Tsai, Chien-Hsiung, Lung-Ming Fu, Chang-Hsien Tai, Yen-Loung Huang, and Jik-Chang Leong. "Computational aero-acoustic analysis of a passenger car with a rear spoiler." *Applied Mathematical Modelling* 33, no. 9 (2009): 3661-3673.
- [6] Kieffer, W., S. Moujaes, and N. Armbya. "CFD study of section characteristics of Formula Mazda race car wings." *Mathematical and Computer Modelling* 43, no. 11-12 (2006): 1275-1287.
- [7] Mitra, D. E. B. O. J. Y. O. T. I. "Effect of relative wind on notch back car with add-on parts." *International Journal of Engineering Science and Technology* 2, no. 4 (2010): 472-476.
- [8] Hu, X. X., and T. T. Wong. "A numerical study on rear-spoiler of passenger vehicle." *World Academy of Science, Engineering and Technology* (2011).

- [9] Hu, X. X., and T. T. Wong. "A numerical study on rear-spoiler of passenger vehicle." *World Academy of Science, Engineering and Technology* (2011).
- [10] Tousi, S. M. R., and P. Bayat. "Evaluating the Importance of Rear Spoiler on Energy Efficiency of Electric Vehicles." *International Journal of Automotive Engineering* 5, no. 4 (2015): 2034-2053.
- [11] Tousi, S. M. R., and P. Bayat. "Evaluating the Importance of Rear Spoiler on Energy Efficiency of Electric Vehicles." *International Journal of Automotive Engineering* 5, no. 4 (2015): 2034-2053.
- [12] Gerhardt, H. J., C. Kramer, Th AmmerschlÄger, and R. Fuhrmann. "Aerodynamic optimization of a group-5 racing car." *Journal of Wind Engineering and Industrial Aerodynamics* 9, no. 1-2 (1981): 155-165.
- [13] Bello-Millán, F. J., T. Mäkelä, L. Parras, C. Del Pino, and C. Ferrera. "Experimental study on Ahmed's body drag coefficient for different yaw angles." *Journal of Wind Engineering and Industrial Aerodynamics* 157 (2016): 140-144.
- [14] Meile, W., T. Ladinek, G. Brenn, A. Reppenhagen, and A. Fuchs. "Non-symmetric bi-stable flow around the Ahmed body." *International Journal of Heat and Fluid Flow* 57 (2016): 34-47.
- [15] Shaharuddin, N.H., Mat Ali, M.S., Mansor, S., Muhamad, S., Shaikh Salim, S.A. and Usman, M. "Flow simulations of generic vehicle model SAE type 4 and DrivAer Fastback using OpenFOAM." *Journal of Advanced Research in Fluid Mechanics and Thermal Sciences* 37 (2017): 18-31.
- [16] Ahmed, Syed R., G. Ramm, and G. Faltin. "Some salient features of the time-averaged ground vehicle wake." *SAE Transactions* 93 (1984): 473-503.
- [17] Cooper, Kevin R. "The effect of front-edge rounding and rear-edge shaping on the aerodynamic drag of bluff vehicles in ground proximity." *SAE Transactions* (1985): 727-757.
- [18] Cheng, S. Y., Makoto Tsubokura, Takuji Nakashima, Takahide Nouzawa, and Yoshihiro Okada. "A numerical analysis of transient flow past road vehicles subjected to pitching oscillation." *Journal of Wind Engineering and Industrial Aerodynamics* 99, no. 5 (2011): 511-522.
- [19] Cheng, S. Y., M. Tsubokura, T. Nakashima, Y. Okada, and T. Nouzawa. "Numerical quantification of aerodynamic damping on pitching of vehicle-inspired bluff body." *Journal of Fluids and Structures* 30 (2012): 188-204.
- [20] Hucho, Wolf-heinich, and Gino Sovran. "Aerodynamics of road vehicles." *Annual review of fluid mechanics* 25, no. 1 (1993): 485-537.